P H Y S I C A L R E V I E W L E T T E R S

Hidden Fermi Liquid, Scattering Rate Saturation, and Nernst Effect: A Dynamical Mean-Field Theory Perspective

Wenhu Xu, Kristjan Haule, and Gabriel Kotliar

Department of Physics and Astronomy, Rutgers University, 136 Frelinghuysen Road, New Jersey 08854, USA
(Received 11 April 2013; published 17 July 2013)

We investigate the transport properties of a correlated metal within dynamical mean-field theory. Canonical Fermi liquid behavior emerges only below a very low temperature scale T_{FL}. Surprisingly the quasiparticle scattering rate follows a quadratic temperature dependence up to much higher temperatures and crosses over to saturated behavior around a temperature scale T_{sat}. We identify these quasiparticles as constituents of the hidden Fermi liquid. The non-Fermi-liquid transport above T_{FL}, in particular the linear-in-T resistivity, is shown to be a result of a strongly temperature dependent band dispersion. We derive simple expressions for the resistivity, Hall angle, thermoelectric power and Nernst coefficient in terms of a temperature dependent renormalized band structure and the quasiparticle scattering rate. We discuss possible tests of the dynamical mean-field theory picture of transport using ac measurements.

Fermi liquids [1] are good conductors. Quasiparticles (QPs) with a mean free path much longer than their wavelength are responsible for the electric transport, and the resistivity vanishes quadratically at low temperatures. The Landau theory is very robust and when reformulated in terms of a transport kinetic equation, it can be used to describe situations where Landau QPs are strictly speaking not well defined, namely when the QP scattering rate is comparable to their energy, such as the electron-phonon coupled system above the Debye temperature [2].

The metallic state of many strongly correlated materials is not described by the Landau theory in a wide range of temperatures. Quadratic temperature dependence of the resistivity occurs in a very narrow or vanishing range of temperatures. The interpretation of the resistivity in terms of the standard model of transport which is based on QPs is problematic since it leads to mean free paths shorter than the (QP) de Broglie wavelength as stressed by Emery and Kivelson [3]. The transport properties of these "bad metals" thus require a novel framework for their theoretical interpretation.

Dynamical mean-field theory (DMFT) [4] provides a nonperturbative framework for the description of strongly correlated materials. It links observable quantities to a simpler, but still interacting, reference system (a quantum impurity in a self-consistent medium) rather than to a free electron system; hence, it gives access to physical regimes outside the scope of the Landau theory.

In a broad temperature range, the single-site DMFT description of the one-band Hubbard model at large U and finite doping results in transport and optical properties with anomalous temperature dependence [5–12], reminiscent of those observed in bad metals. Corresponding studies of half filled metallic systems [13–16] also reveal bad metallic behavior in a narrower temperature region since at high temperatures the resistivity is insulatinglike.

Landau QPs only emerge below an extremely low temperature T_{FL}, which is much lower than the renormalized kinetic energy or Brinkman-Rice scale $T_{\mathrm{BR}} \sim \delta W$ with δ the doping level and W the bare bandwidth. T_{BR} is the natural scale for the variation of physical quantities with doping at zero temperature [7,17]. A recent comprehensive DMFT study of the Hubbard model with a semicircular bare density of states found that the transport properties above T_{FL} are described in terms of resilient QPs with a strong particle-hole asymmetry [11]. This asymmetry arises from the asymmetric pole structure in the self-energy characterizing the proximity to the Mott insulator [18].

In this Letter we investigate the problem of bad metal transport. By expressing the DMFT transport coefficients in terms of QP quantities we find several surprising results: (a) the QP scattering rate has a quadratic behavior for temperatures much larger than T_{FL} and crosses over to a saturated behavior around T_{sat}. (b) The temperature dependence of the transport coefficients is anomalous (in the sense that it does not reflect the T dependence of the QP scattering rate) and arises from the temperature dependent changes of the QP dispersion near the Fermi level. (c) The temperature dependence of the QP dispersion affects differently the diagonal and off-diagonal charge and thermal transport coefficients but the Mott relation [19,20] is valid when $T_{\mathrm{FL}} < T < T_{\mathrm{sat}}/2$.

We study the one-band Hubbard Hamiltonian on the two-dimensional square lattice with nearest neighbor hopping

$$H = -t \sum_{\langle ij \rangle, \sigma} c_{i\sigma}^{\dagger} c_{j\sigma} + U \sum_i c_{i\uparrow}^{\dagger} c_{i\uparrow} c_{i\downarrow}^{\dagger} c_{i\downarrow}. \quad (1)$$

We set the full bare bandwidth $W = 8t$ to $W = 1$ as the unit of energy and temperature, and present results for $U/W = 1.75$, for which the system is a Mott insulator at half filling. The doping level of the metallic state is fixed at

$\delta = 15\%$ ($n = 0.85$). We use the continuous time quantum Monte Carlo (CTQMC) method [21] and the implementation of Ref. [22] to solve the auxiliary impurity problem. We use Padé approximants to analytically continue the self-energy.

The one-electron spectral function is defined as

$$A_{\mathbf{k}}(\omega) = -\frac{1}{\pi} \frac{\mathrm{Im}\Sigma(\omega)}{(\omega + \mu - \epsilon_{\mathbf{k}} - \mathrm{Re}\Sigma(\omega))^2 + \mathrm{Im}\Sigma(\omega)^2}, \quad (2)$$

in terms of the bare band dispersion $\epsilon_{\mathbf{k}} = -(1/4)(\cos(k_x) + \cos(k_y))$ and the self-energy $\Sigma(\omega)$. $A_{\mathbf{k}}(\omega)$ at different temperatures is plotted in Figs. 1(a)–1(d).

Several characteristics of the evolution of $A_{\mathbf{k}}(\omega)$ with temperature are important. The solutions of the following equation

$$\omega + \mu(T) - \epsilon_{\mathbf{k}} - \mathrm{Re}\Sigma(\omega, T) = 0 \quad (3)$$

faithfully reproduce the location of the peaks in $A_{\mathbf{k}}(\omega)$ and how they evolve with temperature [see Fig. 1(f)]. We do not describe in the following the upper Hubbard band at positive energies of order U.

There are two distinct temperature regimes separated by a crossover scale $T_{\mathrm{sat}} \simeq 2T_{\mathrm{BR}}/3 = 0.1$, which also sets the saturation scale of the QP scattering rate as will be explained later. Above T_{sat}, say at $T = 0.125$, $A_{\mathbf{k}}(\omega)$ has one peak, i.e., Eq. (3) has only one root for each $\mathbf{k}$ and displays a continuous dispersion over the whole Brillouin zone. Below T_{sat}, Eq. (3) can have multiple roots. The high temperature band breaks into two parts, which together with the upper Hubbard band form the characteristic DMFT three-peak structure of the local density of states [LDOS, see Fig. 1(e)]. The breakup of these bands also leads to the separation of the optical spectrum into a Drude peak and a midinfrared feature, characteristic of many correlated systems, which provided the earliest experimental tests of the DMFT picture of correlated materials [5,6,13,14].

There is always a dispersive QP feature in an $\sim k_B T$ energy window at the Fermi energy. $\omega_{\mathbf{k}}^*$ denotes the root of Eq. (3) closest to the Fermi level for a given $\mathbf{k}$. It evolves *continuously* with temperature from zero up to very high temperatures where there is no sharp peak in the LDOS [see Fig. 1(e)]. The dispersive excitations evolve continuously from strongly renormalized QPs located near the Luttinger Fermi surface with Fermi crossings around the X point and on the $\Gamma - M$ line for $T \ll T_{\mathrm{sat}}$ [see Figs. 1(a) and 1(b)] to holes in the lower Hubbard band (located near the M point) [see Fig. 1(d)] for $T \gg T_{\mathrm{sat}}$, as the spin degrees of freedom gradually unbind from the charge, with increasing temperature. The QP velocity is nearly temperature independent only below T_{FL} and above T_{sat}. The mass enhancement $(1/Z)$ decreases with increasing temperature, from a large value ~ 5 below T_{FL}
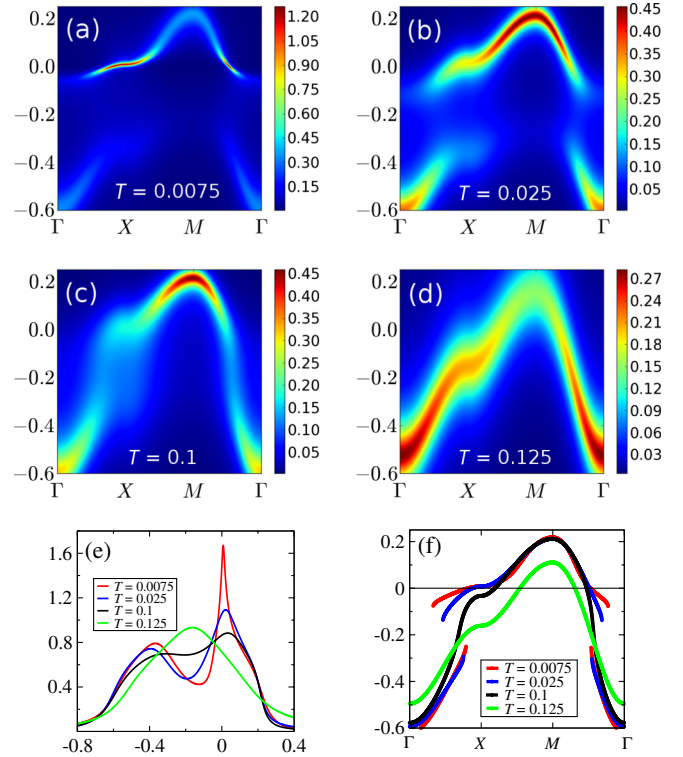

FIG. 1 (color online).   Spectral function $A_{\mathbf{k}}(\omega)$ along $\Gamma - X - M - \Gamma$ in Brillouin zone at (a) $T = 0.0075$, (b) $T = 0.025$, (c) $T = 0.1$, and (d) $T = 0.125$. (e) Local density of states. (f) Roots of Eq. (3) at different temperatures.

[see Fig. 1(a)] to a value $\sim 1.5 \simeq (1 - n/2)^{-1}$ at high temperatures [see Fig. 1(d)].

We now turn to the transport properties and focus on the electric current induced by electric fields and thermal gradients

$$\mathbf{J}_e = \bar{\sigma}^0 \cdot \mathbf{E} - \bar{\sigma}^1 \cdot \boldsymbol{\nabla}\mathrm{T}. \quad (4)$$

$\bar{\sigma}^0$ is the charge conductivity matrix and $\bar{\sigma}^1$ is the thermal conductivity matrix. Several quantities of interest are the resistivity (ρ), Hall angle (θ_H), Seebeck coefficient (S), and Nernst coefficient (ν) [20]. They are representative measures of the magneto- and thermoelectric transport properties and can be expressed in terms of elements of conductivity matrices

$$\rho = \frac{1}{\sigma_{xx}^0}, \qquad \tan\theta_H = -\frac{\sigma_{yx}^0}{\sigma_{xx}^0},$$

$$S = -\frac{\sigma_{xx}^1}{\sigma_{xx}^0}, \qquad \nu = -\frac{1}{B}\left(\frac{\sigma_{yx}^1}{\sigma_{xx}^0} - \frac{\sigma_{xx}^1 \sigma_{yx}^0}{(\sigma_{xx}^0)^2}\right). \quad (5)$$

Within the DMFT treatment of the one-band Hubbard model, current vertex corrections vanish and the transport properties can be interpreted directly in terms of the one-electron spectral function [5,8,9]

$$\sigma_{xx}^{\alpha} = 2\pi \sum_{\mathbf{k}} \Phi_{\mathbf{k}}^{xx} \int d\omega \left(-\frac{\partial f(\omega)}{\partial \omega}\right)\left(\frac{\omega}{T}\right)^{\alpha} A_{\mathbf{k}}^2(\omega),$$

$$\frac{\sigma_{yx}^{\alpha}}{B} = \frac{4\pi^2}{3} \sum_{\mathbf{k}} \Phi_{\mathbf{k}}^{yx} \int d\omega \left(-\frac{\partial f(\omega)}{\partial \omega}\right)\left(\frac{\omega}{T}\right)^{\alpha} A_{\mathbf{k}}^3(\omega),$$

(6)

with $\alpha = 0$ or 1 for charge or thermal conductivity. We consider the limit of a weak magnetic field, hence the off-diagonal conductivities are proportional to B. $\Phi_{\mathbf{k}}^{xx} = \epsilon_{\mathbf{k}}^{x2}$ and $\Phi_{\mathbf{k}}^{yx} = (\epsilon_{\mathbf{k}}^y)^2 \epsilon_{\mathbf{k}}^{xx} - \epsilon_{\mathbf{k}}^y \epsilon_{\mathbf{k}}^x \epsilon_{\mathbf{k}}^{yx}$ are transport functions in terms of the bare band dispersion $\epsilon_{\mathbf{k}}$ and its derivatives. The derivatives are denoted by the corresponding superscripts, $\epsilon_{\mathbf{k}}^{\alpha} = \partial \epsilon_{\mathbf{k}}/\partial k_{\alpha}$.

To recast Eqs. (6) in terms of QPs, we linearize Eq. (3) at $\omega = \omega_{\mathbf{k}}^*$ and define $Z_{\mathbf{k}} = [1 - (\partial \mathrm{Re}\Sigma(\omega)/\partial \omega)]^{-1}|_{\omega=\omega_{\mathbf{k}}^*}$. Then the low energy part of the one-electron Green's function can be approximated as

$$G_{\mathbf{k}}(\omega) \simeq \frac{Z_{\mathbf{k}}}{(\omega - \omega_{\mathbf{k}}^*) + i\Gamma_{\mathbf{k}}^*}.$$

(7)

Thus $Z_{\mathbf{k}}$ is the QP renormalization factor (or QP weight) and $\Gamma_{\mathbf{k}}^* = -Z_{\mathbf{k}}\mathrm{Im}\Sigma(\omega_{\mathbf{k}}^*)$ is the QP scattering rate.

Then the integrals in Eqs. (6) can be performed analytically and lead to

$$\sigma_{xx}^{\alpha} \simeq \sum_{\mathbf{k}} \left(-\frac{\partial f(\omega)}{\partial \omega}\right)_{\omega_{\mathbf{k}}^*} \Phi_{\mathbf{k}}^{*xx}\left(\frac{\omega_{\mathbf{k}}^*}{T}\right)^{\alpha} \tau_{\mathbf{k}}^*,$$

$$\frac{\sigma_{yx}^{\alpha}}{B} \simeq \frac{1}{2}\sum_{\mathbf{k}} \left(-\frac{\partial f(\omega)}{\partial \omega}\right)_{\omega_{\mathbf{k}}^*} \Phi_{\mathbf{k}}^{*yx}\left(\frac{\omega_{\mathbf{k}}^*}{T}\right)^{\alpha} (\tau_{\mathbf{k}}^*)^2.$$

(8)

$\tau_{\mathbf{k}}^* = (\Gamma_{\mathbf{k}}^*)^{-1}$ is the QP lifetime. The transport functions are renormalized by $Z_{\mathbf{k}}$. $\Phi_{\mathbf{k}}^{*xx} = (\epsilon_{\mathbf{k}}^{*x})^2$ and $\Phi_{\mathbf{k}}^{*yx} = (\epsilon_{\mathbf{k}}^{*y})^2 \epsilon_{\mathbf{k}}^{*xx} - \epsilon_{\mathbf{k}}^{*y} \epsilon_{\mathbf{k}}^{*x} \epsilon_{\mathbf{k}}^{*yx}$, with $\epsilon_{\mathbf{k}}^{*\alpha(\beta)} = Z_{\mathbf{k}} \epsilon_{\mathbf{k}}^{\alpha(\beta)}$ ($\alpha, \beta = x, y$).

This reformulation leads to a transparent interpretation in terms of QPs with temperature dependent dispersion $\omega_{\mathbf{k}}^*$. Eqs. (8) have a form similar to the solution of the kinetic equations from Boltzmann theory [23]. The essential difference from the Prange-Kadanoff treatment of the electron-phonon problem [2] is the strong temperature dependence of the QP dispersion brought in by $Z_{\mathbf{k}}$.

First we validate the simplified description of transport, Eqs. (8) ("QP approx."), by benchmarking it against the results of the exact DMFT expressions, Eqs. (6) ("exact exp."), for the resistivity, Hall angle, Seebeck coefficient, and Nernst coefficient. The quantitative agreement between Eqs. (8) and (6) is evident, as shown in Figs. 2(a)–2(d). The QP approximation faithfully reproduces the results of all transport quantities over the whole temperature range, extending to temperatures well above T_{sat}.

Figure 3(a) shows the QP scattering rate on the Fermi surface, i.e., $\Gamma_{\mathbf{k}_F}^*$ with $\omega_{\mathbf{k}_F}^* = 0$ (for later use we also write $\tau_{\mathbf{k}_F}^* = (\Gamma_{\mathbf{k}_F}^*)^{-1}$ as the QP lifetime and $Z_{\mathbf{k}_F}$ as the renormalization factor at the Fermi surface). T_{sat} demarcates the nonmonotonic temperature dependence of $\Gamma_{\mathbf{k}_F}^*$. Below T_{sat}, $\Gamma_{\mathbf{k}_F}^*$ increases and reaches a maximum at T_{sat}. Above T_{sat}, $\Gamma_{\mathbf{k}_F}^*$ decreases very slowly and eventually approaches a value moderately smaller than the maximum. This confirms that T_{sat} characterizes the crossover between two distinct scattering behaviors. The inset of Fig. 3(a) shows estimated values of $(k_F l^*)^{-1}$ with k_F an estimation of the average Fermi momentum by assuming a circular Fermi surface containing $(1 - \delta)/2$ electrons per spin and with $l^* = v_{\mathbf{k}_F}^* \times \tau_{\mathbf{k}_F}^*$ the QP mean free path, where $v_{\mathbf{k}_F}^* = \sqrt{\langle v_{\mathbf{k}}^{*2}\rangle}$ with $\langle \cdots \rangle$ averaging over the Fermi level. At low temperatures, $(k_F l^*)^{-1}$ increases with temperature, as expected in a good metal, and crosses over to a much slower increase, or saturated behavior, around $T_{\mathrm{sat}}/2$. Above $T_{\mathrm{sat}}/2$, $(k_F l^*)^{-1} \simeq 0.5$, and does not exceed the Mott-Ioffe-Regel bound, which states that $(k_F l^*)^{-1} < 1$ in a metal. The QPs behave as expected in Boltzmann transport theory in the full temperature range, reaching the nondegenerate limit at $T \gg T_{\mathrm{sat}}$. Notice that above T_{FL}, $\mathrm{Im}\Sigma(0)$ is not quadratic in temperature; only $\Gamma_{\mathbf{k}_F}^* = -Z_{\mathbf{k}_F}\mathrm{Im}\Sigma(0)$ is quadratic.

The anomalies in the transport properties are the result of the strong temperature dependence of the renormalized dispersion. This is best understood by means of a general Sommerfeld expansion of Eqs. (8), which is explained in the Supplemental Material [24] and works well below $T_{\mathrm{sat}}/2$. For this purpose we define
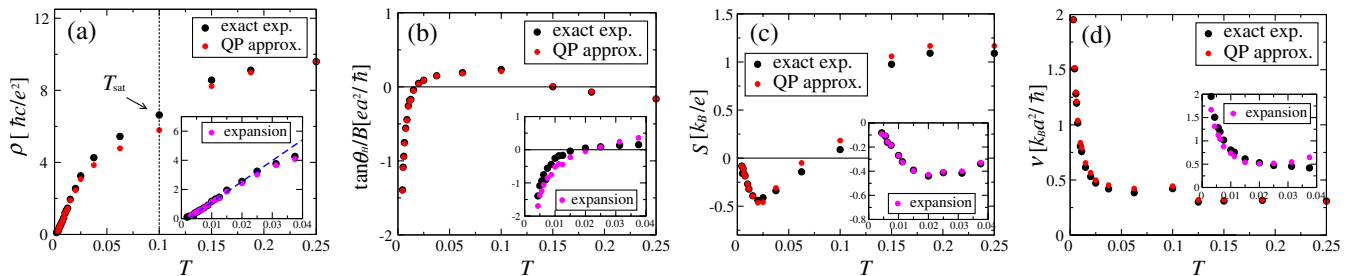

FIG. 2 (color online).   Transport properties. (a) Resistivity. (b) Hall angle. (c) Seebeck coefficient. (d) Nernst coefficient. Points labeled "exact exp." are obtained using Eqs. (6). Points labeled "QP approx." are obtained using Eqs. (8). Points labeled "expansion" are obtained using the general Sommerfeld expansion detailed in Supplemental Material [24]. The units are expressed in terms of universal constants, $\hbar$, k_B, e, the in-plane lattice constant a, and the out-of-plane lattice constant c.
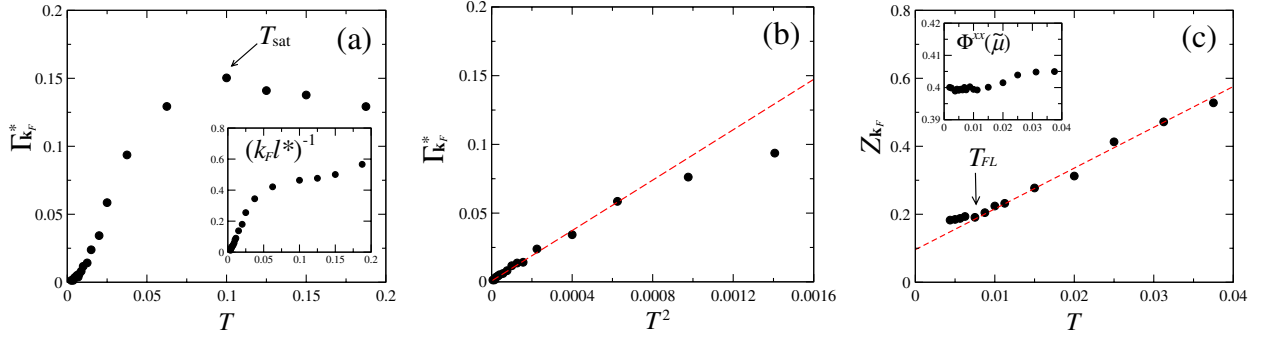
FIG. 3 (color online). (a) Quasiparticle scattering rate $\Gamma^*_{\mathbf{k}_F}$. The inset shows the estimation of $(k_F l^*)^{-1}$. (b) $\Gamma^*_{\mathbf{k}_F}$ as a function of T^2 for $T \lesssim T_{\text{sat}}/2$. (c) Quasiparticle renormalization factor $Z_{\mathbf{k}_F}$ for $T \lesssim T_{\text{sat}}/2$.

$\Phi^{*xx/yx}(\epsilon) = \sum_{\mathbf{k}} \Phi^{*xx/yx}_{\mathbf{k}} \delta(\epsilon - \omega^*_{\mathbf{k}})$ and the energy dependent QP lifetime $\tau^*(\epsilon) = \tau^*_{\mathbf{k}}$ when $\epsilon = \omega^*_{\mathbf{k}}$, with scattering rate $\Gamma^*(\epsilon) = (\tau^*(\epsilon))^{-1}$. For $|\epsilon| \lesssim T$, $\Phi^{*xx/yx}(\epsilon)$ is expanded to linear order in ϵ. To keep the asymmetry in $\Gamma^*(\epsilon)$, which is important for the thermoelectric transport, we expand $\Gamma^*(\epsilon)$ to cubic order in ϵ, and treat the linear and cubic order as corrections to the zeroth and quadratic terms, which are dominant in the Fermi liquid regime at low temperatures. The insets in Fig. 2 compare the estimation using this expansion (purple dots) and the results of the full expressions (black dots). The agreement is evident and the expansion quantitatively captures the variation below $T_{\text{sat}}/2$.

The inset of Fig. 2(a) shows the linearity of the resistivity, a typical non-Fermi-liquid behavior [25], up to $T_{\text{sat}}/4 \simeq 0.025$, as indicated by the linear fitting (blue dashed line). Surprisingly the QP scattering rate $\Gamma^*_{\mathbf{k}_F}$ has a quadratic temperature dependence also up to $T_{\text{sat}}/4$ [see Fig. 3(b)]. This is due to the strong temperature dependence of $Z_{\mathbf{k}_F}$ [see Fig. 3(c)]. In fact, the leading order in the general Sommerfeld expansion gives

$$\rho \simeq (Z_{\mathbf{k}_F} \Phi^{xx}(\tilde{\mu}) \tau^*_{\mathbf{k}_F})^{-1}, \qquad (9)$$

where $\Phi^{xx}(\tilde{\mu}) = \sum_{\mathbf{k}} \Phi^{xx}_{\mathbf{k}} \delta(\tilde{\mu} - \epsilon_{\mathbf{k}})$ with $\tilde{\mu} = \mu - \text{Re}\Sigma(0)$ and we have used $\Phi^{*xx}(0) = Z_{\mathbf{k}_F} \Phi^{xx}(\tilde{\mu})$. $Z_{\mathbf{k}_F} \simeq 0.1 + 12T$ for $T_{\text{FL}} < T < T_{\text{sat}}/4$ leads to the quasilinear resistivity and also affects all other transport coefficients in Eqs. (8). The temperature dependence of $Z_{\mathbf{k}_F}$ becomes negligible only below the Fermi liquid temperature $T_{\text{FL}} \simeq T_{\text{sat}}/15$. $\Phi^{xx}(\tilde{\mu})$ is very weakly temperature dependent as shown in the inset of Fig. 3(c). Above T_{sat}, the resistivity is quasilinear in temperature with a slope smaller than that below $T_{\text{sat}}/4$, while the QP scattering rate is saturated. The general Sommerfeld expansion cannot be used at high temperatures, but the discrepancy between the scattering rate and resistivity can be traced to the variation of $\tilde{\mu}$ with temperature, leading to the shift of the QP band relative to the Fermi window $-\partial f(\omega)/\partial \omega$.

Similarly, the leading order in the Hall angle [see Fig. 2(b)] is given by $\tan\theta_H/B \simeq Z_{\mathbf{k}_F} \Phi^{yx}(\tilde{\mu}) \tau^*_{\mathbf{k}_F}/2\Phi^{xx}(\tilde{\mu})$

and indicates that the sign change at $T \simeq T_{\text{sat}}/4$ is due to the sign change in $\Phi^{yx}(\tilde{\mu})$, a consequence of the evolution of Fermi surface from a holelike one to an electronlike one. For the Seebeck coefficient [see Fig. 2(c)], the expansion leads to

$$S \simeq \left(-\frac{\pi^2}{3}T\right)\left(\frac{d\ln\Phi^{*xx}(0)}{d\epsilon} + \frac{d\ln\tau^*(0)}{d\epsilon}\right). \qquad (10)$$

The asymmetry in the scattering rate competes with the asymmetry in the QP band structure; hence, instead of a sign change, S shows a nonmonotonic temperature dependence below $T_{\text{sat}}/2$.

The Nernst coefficient ν [see Fig. 2(d)] rises steeply below $T_{\text{sat}}/4$, and provides a good probe of the temperature dependence of $\tau^*_{\mathbf{k}_F}$. The leading orders in the expansion give

$$\nu \simeq \left(-\frac{\pi^2}{3}T\right)\left[\tau^*_{\mathbf{k}_F}\frac{d}{d\epsilon}\left(\frac{\Phi^{*yx}(0)}{\Phi^{*xx}(0)}\right) + \frac{\Phi^{*yx}(0)}{\Phi^{*xx}(0)}\frac{d\tau^*(0)}{d\epsilon}\right]. \qquad (11)$$

In the square lattice near hall filling, the asymmetry in the band structure dominates and leads to $\nu \propto \tau^*_{\mathbf{k}_F}T \propto 1/T$. This rise is seen in many materials [20] before ν drops linearly in T at very low temperature [26].

Further studies should be carried out to ascertain to which extent the DMFT description of transport applies to real materials, but the strong similarities between the experimental features revealed in the phenomenological picture in Ref. [25] and our results are encouraging. Alternating current (ac) transport measurements can be used to extract the temperature dependence of $\tau^*_{\mathbf{k}_F}$. At low frequency, the optical conductivity is parametrized as [27,28] $\sigma(\omega) = (\omega^{*2}_{\text{opt}}/4\pi)[-i\omega + (1/\tau^*_{\text{opt}})]^{-1}$, with $\omega^{*2}_{\text{opt}} \simeq 8\pi\Phi^{*xx}(0) = 8\pi Z_{\mathbf{k}_F}\Phi^{xx}(\tilde{\mu})$ and $\tau^*_{\text{opt}} \simeq \tau^*_{\mathbf{k}_F}/2$. Similarly in the ac Hall effect [29], $\tan\theta_H(\omega)/B = (\omega^{*2}_H/4\pi)[-i\omega + (1/\tau^*_H)]^{-1}$ follows, with

$$\omega^{*2}_H \simeq 4\pi\frac{\Phi^{*yx}(0)}{\Phi^{*xx}(0)} = 4\pi\frac{Z_{\mathbf{k}_F}\Phi^{yx}(\tilde{\mu})}{\Phi^{xx}(\tilde{\mu})}$$

and $\tau_H^* \simeq \tau_{\mathbf{k}_F}^*/2$. Frequency dependent thermoelectric measurements would give additional information on the asymmetry of the QP dispersion and scattering rate.

The extension from model Hamiltonians to the LDA + DMFT framework is straightforward. It can be used to separate the temperature dependence of transport coefficients arising from the temperature dependence of the QP band and that of the scattering rate, in materials such as the ruthenates [30], the vanadates [31], and the nickelates [14,32,33] for which the LDA + DMFT description is known to provide an accurate zeroth order picture of numerous properties [14]. Recent experiments on cuprates [34] have revealed evidence for the temperature dependence of $\omega_{\rm opt}^{*2}$ and a T^2-scattering rate over a broad range of temperatures. These materials require cluster DMFT studies to describe their momentum space differentiation. Still, it is tempting to interpret the transport properties in terms of QPs to provide an effective description of the transport. Indeed the QP scattering rate computed in the t-J model in Ref. [35], exhibits the saturation behavior described in this work and it would be interesting to reanalyze the results in terms of the QPs of the hidden Fermi liquid. Our findings are related to two earlier theoretical proposals. Anderson introduced the idea of a hidden Fermi liquid [36,37], requiring $Z_{\mathbf{k}_F}$ to strictly vanish at $T = 0$ in the normal state. Alternatively, our results could be cast into the framework of the extremely correlated Fermi liquid [38] by the temperature dependence of the caparison function.

[1] L. Landau, Sov. Phys. JETP **3**, 920 (1957).
[2] R. E. Prange and L. P. Kadanoff, Phys. Rev. **134**, A566 (1964).
[3] V. J. Emery and S. A. Kivelson, Phys. Rev. Lett. **74**, 3253 (1995).
[4] A. Georges, G. Kotliar, W. Krauth, and M. J. Rozenberg, Rev. Mod. Phys. **68**, 13 (1996).
[5] T. Pruschke, D. L. Cox, and M. Jarrell, Phys. Rev. B **47**, 3553 (1993).
[6] T. Pruschke, M. Jarrell, and J. Freericks, Adv. Phys. **44**, 187 (1995).
[7] H. Kajueter, G. Kotliar, and G. Moeller, Phys. Rev. B **53**, 16214 (1996).
[8] G. Pálsson and G. Kotliar, Phys. Rev. Lett. **80**, 4775 (1998).
[9] E. Lange and G. Kotliar, Phys. Rev. B **59**, 1800 (1999).
[10] W. Xu, C. Weber, and G. Kotliar, Phys. Rev. B **84**, 035114 (2011).
[11] X. Deng, J. Mravlje, R. Zitko, M. Ferrero, G. Kotliar, and A. Georges, Phys. Rev. Lett. **110**, 086401 (2013).
[12] L.-F. Arsenault, B. S. Shastry, P. Sémon, and A.-M. S. Tremblay, Phys. Rev. B **87**, 035126 (2013).
[13] M. J. Rozenberg, G. Kotliar, H. Kajueter, G. A. Thomas, D. H. Rapkine, J. M. Honig, and P. Metcalf, Phys. Rev. Lett. **75**, 105 (1995).
[14] J. Merino and R. H. McKenzie, Phys. Rev. B **61**, 7996 (2000).
[15] P. Limelette, P. Wzietek, S. Florens, A. Georges, T. A. Costi, C. Pasquier, D. Jérome, C. Mézière, and P. Batail, Phys. Rev. Lett. **91**, 016401 (2003).
[16] J. Merino, M. Dumm, N. Drichko, M. Dressel, and R. H. McKenzie, Phys. Rev. Lett. **100**, 086404 (2008).
[17] D. S. Fisher, G. Kotliar, and G. Moeller, Phys. Rev. B **52**, 17112 (1995).
[18] P. Grete, S. Schmitt, C. Raas, F. B. Anders, and G. S. Uhrig, Phys. Rev. B **84**, 205104 (2011).
[19] M. Jonson and G. D. Mahan, Phys. Rev. B **21**, 4223 (1980).
[20] K. Behnia, J. Phys. Condens. Matter **21**, 113101 (2009).
[21] P. Werner, A. Comanac, L. de' Medici, M. Troyer, and A. J. Millis, Phys. Rev. Lett. **97**, 076405 (2006).
[22] K. Haule, Phys. Rev. B **75**, 155113 (2007).
[23] N. W. Ashcroft and N. D. Mermin, *Solid State Physics* (Saunders, Philadelphia, 1976).
[24] See Supplemental Material at http://link.aps.org/supplemental/10.1103/PhysRevLett.111.036401 for the derivation of the general Sommerfeld expansion.
[25] N. Hussey, K. Takenaka, and H. Takagi, Philos. Mag. **84**, 2847 (2004).
[26] Disorder in real materials cuts off the divergence of $\tau_{\mathbf{k}_F}^*$ and ν is thus linear in T at very low temperatures. This linearity is sometimes taken as a signature of Fermi-liquid behavior.
[27] D. van der Marel, H. J. A. Molegraaf, J. Zaanen, Z. Nussinov, F. Carbone, A. Damascelli, H. Eisaki, M. Greven, P. Kes, and M. Li, Nature (London) **425**, 271 (2003).
[28] D. N. Basov, R. D. Averitt, D. van der Marel, M. Dressel, and K. Haule, Rev. Mod. Phys. **83**, 471 (2011).
[29] H. Drew, S. Wu, and H. S. Lihn, J. Phys. Condens. Matter **8**, 10037 (1996).
[30] J. Mravlje, M. Aichhorn, T. Miyake, K. Haule, G. Kotliar, and A. Georges, Phys. Rev. Lett. **106**, 096401 (2011).
[31] R. Arita, K. Held, A. V. Lukoyanov, and V. I. Anisimov, Phys. Rev. Lett. **98**, 166402 (2007).
[32] M. K. Stewart, C.-H. Yee, J. Liu, M. Kareev, R. K. Smith, B. C. Chapler, M. Varela, P. J. Ryan, K. Haule, J. Chakhalian *et al.*, Phys. Rev. B **83**, 075125 (2011).
[33] X. Deng, M. Ferrero, J. Mravlje, M. Aichhorn, and A. Georges, Phys. Rev. B **85**, 125137 (2012).
[34] S. I. Mirzaei, D. Stricker, J. N. Hancock, C. Berthod, A. Georges, E. van Heumen, M. K. Chan, X. Zhao, Y. Li, M. Greven *et al.*, arXiv:1207.6704.
[35] K. Haule and G. Kotliar, Phys. Rev. B **76**, 104509 (2007).
[36] P. W. Anderson, Phys. Rev. B **78**, 174505 (2008).
[37] P. A. Casey and P. W. Anderson, Phys. Rev. Lett. **106**, 097002 (2011).
[38] B. S. Shastry, Phys. Rev. Lett. **107**, 056403 (2011).